Chemical Variations of Pyroxene and Fe-Ti–Oxide Crystals in Basalts Hosting Cu-Au Porphyry Mineralization in the Quesnel Terrane, Interior British Columbia (NTS 092H, I, P, 093A, J, N)

S. Vaca, Mineral Deposit Research Unit, University of British Columbia, Vancouver, BC, svaca@eos.ubc.ca

T. Bissig, Mineral Deposit Research Unit, University of British Columbia, Vancouver, BC

M. Raudsepp, Department of Earth and Ocean Sciences, University of British Columbia, Vancouver, BC

C.J.R. Hart, Mineral Deposit Research Unit, University of British Columbia, Vancouver, BC

Vaca, S., Bissig, T., Raudsepp, M. and Hart, C.J.R. (2012): Chemical variations of pyroxene and Fe-Ti–oxide crystals in basalts hosting Cu-Au porphyry mineralization in the Quesnel terrane, interior British Columbia (NTS 092H, I, P, 093A, J, N); *in* Geoscience BC Summary of Activities 2011, Geoscience BC, Report 2012-1, p. 69–78.

Introduction

The Late Triassic Quesnel terrane is mainly composed of rocks of the Nicola Group and its along-strike equivalent Takla Group, both of which are largely composed of alkalic and lesser calcalkalic basalts, derivative volcanic products and associated arc-fringing sedimentary strata (Dawson, 1879; Preto, 1979; Mortimer, 1987). Hereafter, these two groups are referred to as the Nicola Group. The Quesnel terrane in British Columbia is known to host several alkalic porphyry Cu-Au deposits, including (from north to south) Lorraine, Mount Milligan, Mount Polley, Afton/Ajax and Copper Mountain (Figure 1).

Variation in the magnetic susceptibility values and Fe^{2+}/Fe^{3+} ratios in basalts from different localities in central Quesnel terrane have been previously documented by Bissig et al. (2010) and Vaca et al. (2011). These authors showed that the volcanic arc can be subdivided on the basis of variation in oxidation state and magnetic susceptibility. Porphyry Cu-Au deposits broadly coeval with volcanism at Mount Polley are hosted in a relatively oxidized and alkaline part of the arc when compared to areas devoid of coeval porphyry style of mineralization. Although the least altered basalts were studied, the magnetic susceptibility and Fe^{3+} content may be influenced by low temperature alteration processes. Thus, in this paper we present an alternate way to estimate oxidation state and alkalinity of magmas using the chemistry of effectively unaltered phenocrysts.

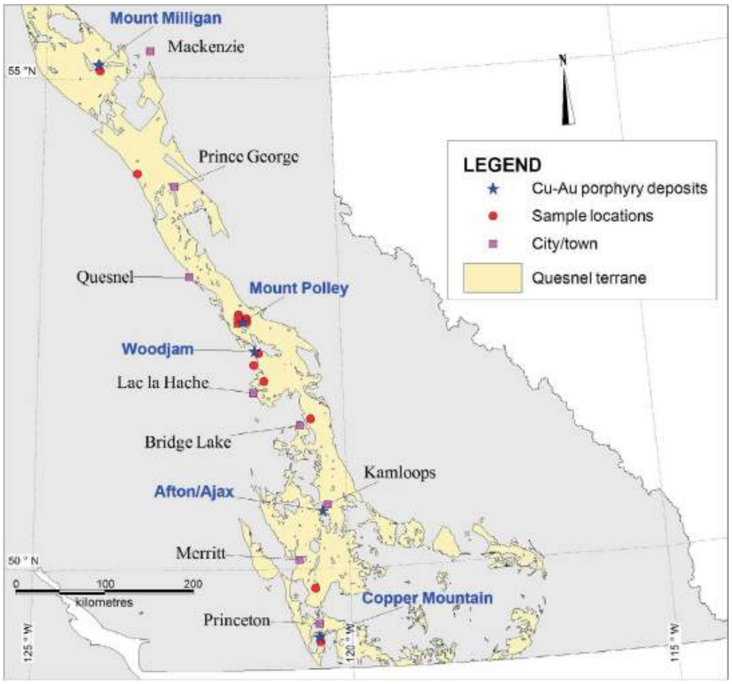

Figure 1. Spatial distribution of Cu-Au porphyry deposits in the Quesnel terrane of interior British Columbia (the Lorraine deposit is located north of the area covered by the figure).

Clinopyroxene is the most common phenocryst in basalts of the Quesnel terrane. Pyroxenes from different Nicola Group map units around the Mount Polley Cu-Au porphyry deposit (Logan and Bath, 2005; Logan et al., 2007) were selected for microanalytical geochemistry. Clinopyroxene compositions from these areas were compared with those from other localities, along strike but still within the arc (Figure 1).

Scanning electron microscopy (SEM) and electron microprobe (EMP) analyses were performed to obtain qualitative and quantitative analyses of the chemical variations within and between pyroxene crystals. In addition, the composi-

---

Keywords: *Nicola Group, alkalic porphyry, microprobe, pyroxene, basalt*

This publication is also available, free of charge, as colour digital files in Adobe Acrobat® PDF format from the Geoscience BC website: http://www.geosciencebc.com/s/DataReleases.asp.

tion of the Fe-Ti–oxide inclusions within pyroxene was determined.

Pyroxene and Fe-Ti–oxide chemistry records the alkalinity and oxidation state of parent magma (Kushiro, 1960; LeBas, 1962; Taylor, 1964). High oxidation state is an important characteristic of igneous rocks related to porphyry Cu-Au mineralization (e.g., Seedorff et al., 2005; Chamberlain et al., 2007). Thus, studying chemical changes of minerals within basalts will lead to a more complete understanding of the magmatic evolution of the arc. This might generate new ideas on the prospectivity for comagmatic Cu-Au porphyry mineralization in different arc segments.

Samples

Sampling was conducted during the 2009 and 2010 summer field seasons and was focused on coherent volcanic rocks from different localities along the Quesnel terrane (Figure 1).

The areas studied in this research include

- Mount Polley, where host volcanic rocks are interpreted to be broadly coeval with the mineralization (Bailey and Hodgson, 1979; Logan and Bath, 2005); three different map units of volcanic host rocks around this alkalic silica-undersaturated Cu-Au porphyry deposit were sampled (see Figure 2);
- Mount Milligan, where basaltic host rocks are cut by silica-saturated alkalic porphyry Cu-Au mineralization that is approximately 20 m.y. younger (Nelson and Bellefontaine, 1996);
- Copper Mountain, where silica-saturated alkalic Cu-Au porphyry deposits are interpreted to be coeval with the volcanic host rocks, paleontological data of the south-

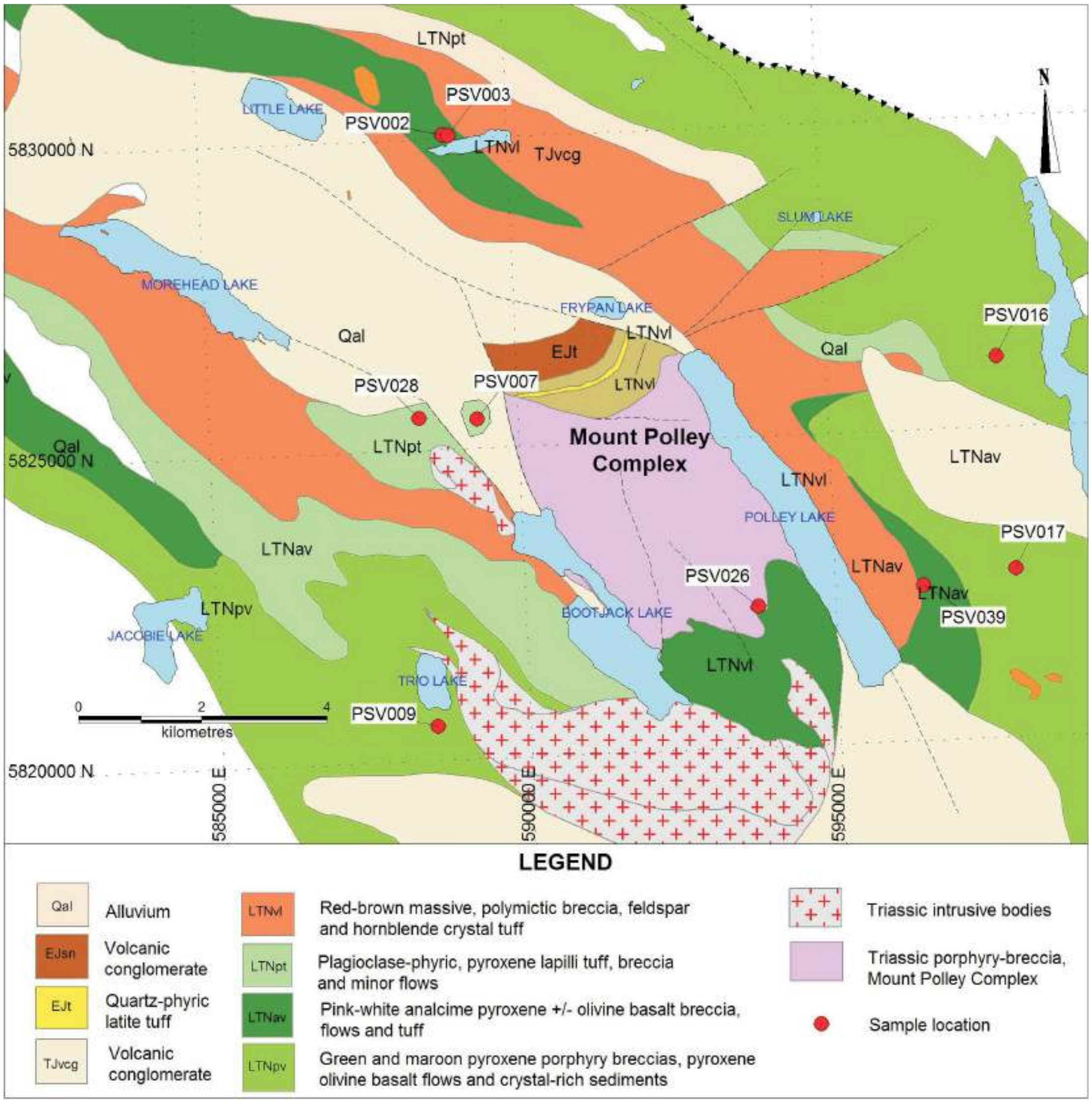

Figure 2. Different map units at the Mount Polley area, showing the location of the samples used in this research (Modified from Logan et al., 2007).

eastern part of the Nicola Group is Late Norian, ca. 204 Ma and intrusive bodies in the Copper Mountain complex date to ca. 200–205 Ma (Carter et al., 1991; Mortensen et al., 1995);

- Woodjam prospect, which features silica-saturated porphyry Cu-Au-Mo mineralization; recent detailed mapping by Blackwell et al. (2010) revealed that a rock unit previously mapped as a plagioclase porphyry stock is actually part of the volcanic succession, presenting an age of ca. 204 Ma, while the age of the intrusion is ca. 196.84 Ma (Schiarizza unpublished zircon ages in Logan et al., 2011), thus, volcanic rocks here are approximately 7 m.y. older than the fertile intrusions;
- Lac la Hache prospect, where Cu-Au mineralization is interpreted to be related to alkalic intrusions (Schiarizza et al., 2008), both host rock and mineralization ages are unknown; and
- exposures around Prince George, Bridge Lake and south of Merritt, that represent apparently barren arc segments (Figure 1).

Analytical Procedures

Magnetic susceptibility was measured in the field using a KT-9 Kappameter handheld instrument. The values reported are the average of 10 readings over the outcrop. Polished thin sections were prepared from 17 rock samples from different locations in the study area, for petrography, SEM and EMP analyses. All analyses were conducted in the laboratories at the Department of Earth and Ocean Sciences, University of British Columbia.

Detailed petrographic observations were made using transmitted and reflected light microscopy. Polished thin sections were carbon coated in an Edwards Auto 306 carbon-coater instrument. The SEM analyses were done with a Philips™ XL-30 scanning electron microscope/Bruker Quanta™ 200 energy-dispersion X-ray microanalysis system. Chemical compositions of pyroxene and Fe-Ti oxides were determined using a fully automated CAMECA™ SX-50 electron microprobe. Pyroxene compositions were measured with the following operating conditions: excitation voltage, 15 kV; beam current, 20 nA; peak count-time, 20 s; background count-time, 10 s; spot diameter, 5 μm. The Fe-Ti–oxide analyses were obtained using the same operating conditions as pyroxene. Standards for pyroxene and Fe-Ti–oxide analyses are indicated in Table 1.

Data reduction for was done using the 'PAP' $\phi(\rho Z)$ method (Pouchou and Pichoir, 1985). The structural formulas of pyroxene were calculated on the basis of 6 O; for Fe-Ti oxides, structural formulas were calculated on the basis of 32 O. The Fe^{3+} content was calculated using the method proposed by Droop (1987).

Petrography

Detailed petrographic study shows that all samples are basalts, except for one sample collected from the Woodjam property, which is a basaltic andesite. The rocks are porphyritic, with a visual estimation of 30–60% phenocrysts per sample, ranging from 1 to 5 mm in diameter. Phenocrysts are mainly euhedral to subhedral clinopyroxene, tabular plagioclase and, in the most alkaline basalts, euhedral to anhedral analcime is present. Mineral proportions vary according to sample location as demonstrated in Table 2. Groundmass in all samples consists of fine-grained plagioclase, clinopyroxene, opaque minerals and products of volcanic glass devitrification.

The rocks are weakly altered, with a chlorite-calcite-epidote assemblage, overprinting the fine-grained groundmass; hematite is also locally present.

Scanning Electron Microscopy and Electron Microprobe Analyses

Clinopyroxene

In all samples, clinopyroxene crystals are colourless to pale green in transmitted light, ≤4 mm, euhedral to subhedral,

Table 1. Standards, analysis lines and crystals used for pyroxene and Fe-Ti–oxide analyses.

Pyroxene	Fe-Ti oxides
albite, $Na_{K\alpha}$, TAP	synthetic spinel, $Al_{K\alpha}$, TAP
kyanite, $Al_{K\alpha}$, TAP	synthetic magnesiochromite, $Mg_{K\alpha}$, TAP
diopside, $Mg_{K\alpha}$, TAP	diopside, $Si_{K\alpha}$, TAP
diopside, $Si_{K\alpha}$, TAP	diopside, $Ca_{K\alpha}$, PET
diopside, $Ca_{K\alpha}$, PET	rutile, $Ti_{K\alpha}$, PET
rutile, $Ti_{K\alpha}$, PET	synthetic magnesiochromite, $Cr_{K\alpha}$, LIF
synthetic magnesiochromite, $Cr_{K\alpha}$, LIF	synthetic rhodonite, $Mn_{K\alpha}$, LIF
synthetic rhodonite, $Mn_{K\alpha}$, LIF	synthetic fayalite, $Fe_{K\alpha}$, LIF
synthetic fayalite, $Fe_{K\alpha}$, LIF	synthetic Ni_2SiO_4, $Ni_{K\alpha}$, LIF
synthetic Ni_2SiO_4, $Ni_{K\alpha}$, LIF	vanadium metal, $V_{K\alpha}$, PET

Abbreviations: LIF, lithium fluoride; PET, pentaerythritol; TAP, thallium acid phthalate

Table 2. List of samples showing the amounts of the most important phenocryst phases and the occurrence of Fe-Ti oxides and hematite within the basalts. Magnetic-susceptibility values indicate the presence and amount of magnetite. All of the samples have been affected by weak epidote-chlorite-calcite alteration.

Sample ID	UTM: NAD 83, Zone 10S		Location	Main phenocryst phases			Fe-Ti oxide (%)	Hem[1]	Magnetic susceptibility[2] (SI units)
	Easting	Northing		Cpx (%)	Plag (%)	Anl (%)			
PSV002	588966	5830062	Mount Polley-LTNav	30	14	12	1	x	21.5
PSV003	589059	5830056	Mount Polley-LTNav	30	15		1		41.9
PSV007	589328	5825476	Mount Polley-LTNpt	10	50		1 2		70.1
PSV009	588497	5820559	Mount Polley-LTNpv	25	35		1 2		70
PSV016	597756	5826139	Mount Polley-LTNpv	25	4		1		23.7
PSV017	597925	5822708	Mount Polley-LTNpv	30	3	7	<1	x	1.16
PSV026	593744	5822273	Mount Polley-LTNav	35	25		2 3		86.1
PSV028	588392	5825520	Mount Polley-LTNpt	20	30		2 3		111
PSV039	596426	5822502	Mount Polley-LTNav	20	15	30	1 2	x	60.9
MTB031	433079	6105548	Mount Milligan	27	5		<1		0.4
CMSV203	681762	5461207	Copper Mountain	40	5		<1		1.2
WTB085	611019	5786299	Woodjam	25	30		1	x	1.55
LTB073	606030	5773254	Lac la Hache north	33	13		1 2		83.5
LTB067	617760	5755186	Lac la Hache south	35	25		2	x	40
PGTB074	474874	5989106	Prince George	12	30		<1		15.4
BTB051	670097	5712526	Bridge Lake	37	5		<1		1.29
SSV128	676083	5521435	South of Merritt	25	5	10	1	x	0.27

[1] within the matrix (primary and/or alteration)

[2] values are multiplied by 10^{-3} (e.g., 21.50 x $10^{-3)}$

Abbreviations: Anl, analcime; Cpx, clinopyroxene; Hem, hematite; Plag, plagioclase

and typically display concentric zonation. Magnetite and apatite inclusions are common (Figure 3). They are variably fractured and locally chloritized, but only effectively unaltered crystals were analyzed in this study. Generally, clinopyroxene spans a narrow overall chemical variation from core to rim. The average composition of the pyroxene phenocrysts in basalts along the Quesnel terrane is $(Ca_{0.89},Fe^{2+}_{0.08},Na_{0.03})(Al^{VI}_{0.03},Fe^{3+}_{0.11},Fe^{2+}_{0.05},Ti_{0.02},Mg_{0.79},Mn_{0.01})(Si_{1.85,}Al^{IV}_{0.15})O_6$, falling in the diopside field of the pyroxene quadrilateral (Figure 4). Most analyses plot in the diopside field, except for some data from the Mount Polley, Prince George and Woodjam areas, which straddle the border of the augite field (Figure 4).

Pyroxene compositions comprise two populations (Figure 4). The more crowded population (right) ranges between 10–20 mol % Fe content and corresponds to analyses performed from core through interior to rim in the crystals from all localities, except Woodjam. The other population (left, circled by brown dashed line) lies within 0–10 mol %

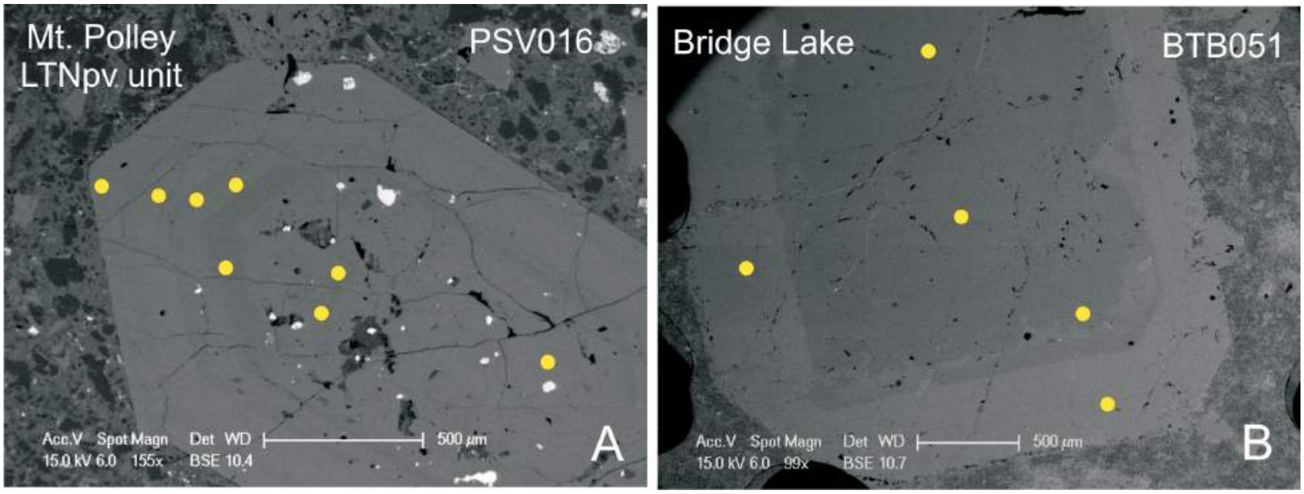

Figure 3. Representative backscattered electron images of clinopyroxene, electron microprobe (EMP) analysis spots are shown in yellow: **A)** clinopyroxene showing concentric zonation and Fe-Ti–oxide inclusions (bright gray); **B)** zoned clinopyroxene evidencing a sharp transition between the core/interior (dark gray) and rim (light gray). Note that magnetite inclusions are present only within pyroxene A. Zonation suggests rapid changes in the temperature-composition (T-X) parameters during crystallization.

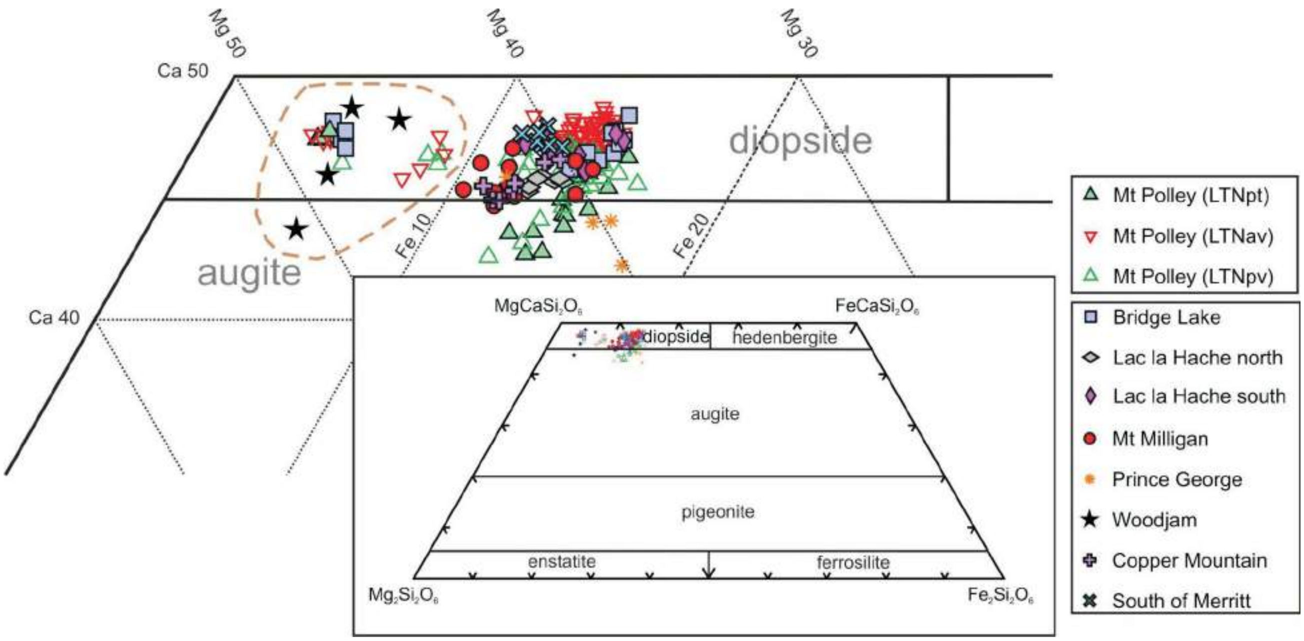

Figure 4. Pyroxene quadrilateral compositions for basalts of the Quesnel terrane. The circled field corresponds to pyroxene from core to rim of the Woodjam sample, and some spots from cores and interiors of pyroxene crystals from samples collected near Bridge Lake and Mount Polley. The pyroxene quadrilateral is that of Morimoto (1988).

Fe, and includes the Woodjam sample and some spots from cores and interiors only (no rims) of the Bridge Lake sample and Mount Polley samples (PSV007, PSV016, PSV017, PSV026 and PSV039, refer to Figure 2).

Chemical composition of pyroxene is characterized by a nearly constant Ca content of ~0.9 cations per formula unit (cpfu); the Mg# ($100*Mg^{2+}/(Mg^{2+}+Fe^{2+})$) ranges from 76.27 to 98.12, showing an overlap among the different rock units (Figure 5). Most spot analyses from Copper Mountain, Lac la Hache north, South of Merritt and unit LTNav at Mount Polley fall above an empirically defined division line at Mg# of 85, whereas pyroxene from Mount Milligan, Lac la Hache south, Bridge Lake, Prince George and unit LTNpt at Mount Polley fall mostly below this line. Analy-

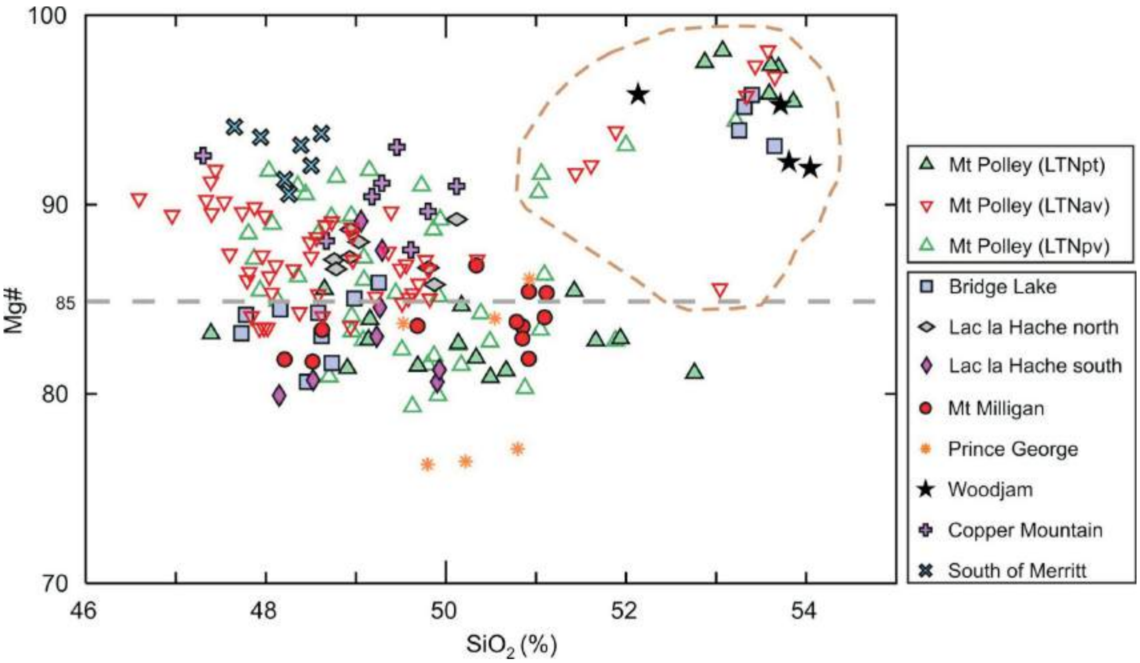

Figure 5. Chemical distribution based on the content of SiO$_2$ and Mg# from electron microprobe (EMP) analyses of pyroxene crystals in basalts of the Nicola Group. High Mg# is indicative of primitive melts. Dashed brown line outlines pyroxene analyses from Woodjam, with some core and interior analyses from Bridge Lake and Mount Polley.

ses from the unit LTNpv plot both above and below this reference line.

Another group of spots with high Mg# (85.56–98.12) and SiO_2 (51.03–54.05%) content (Figure 5, top right, dashed brown line) corresponds to core and interiors of pyroxene analyses from Woodjam and some from Bridge Lake and Mount Polley. This group matches with the group with lower Fe values in Figure 4. Pyroxene crystals contain sufficient Si and Al to fill the tetrahedral site (Al^{IV}), except for a few analyses from Bridge Lake and Mount Polley samples, which require addition of Fe^{3+} (0.03–0.018 cpfu). This group also coincides with the analyses outlined in the Figure 4 (top left) and Figure 5 (top right).

Overall calculated Fe^{3+} within clinopyroxene present values ranging from 0.002 to 0.19 cpfu and Al^{IV} numbers between 0.006 and 0.25 cpfu (Figure 6A); overlap among the different localities is common, however, some trends in the data can be recognized. Pyroxene from Copper Mountain, Bridge Lake, Lac la Hache north, units LTNav and LTNpv at Mount Polley and south of Merritt have a consistently

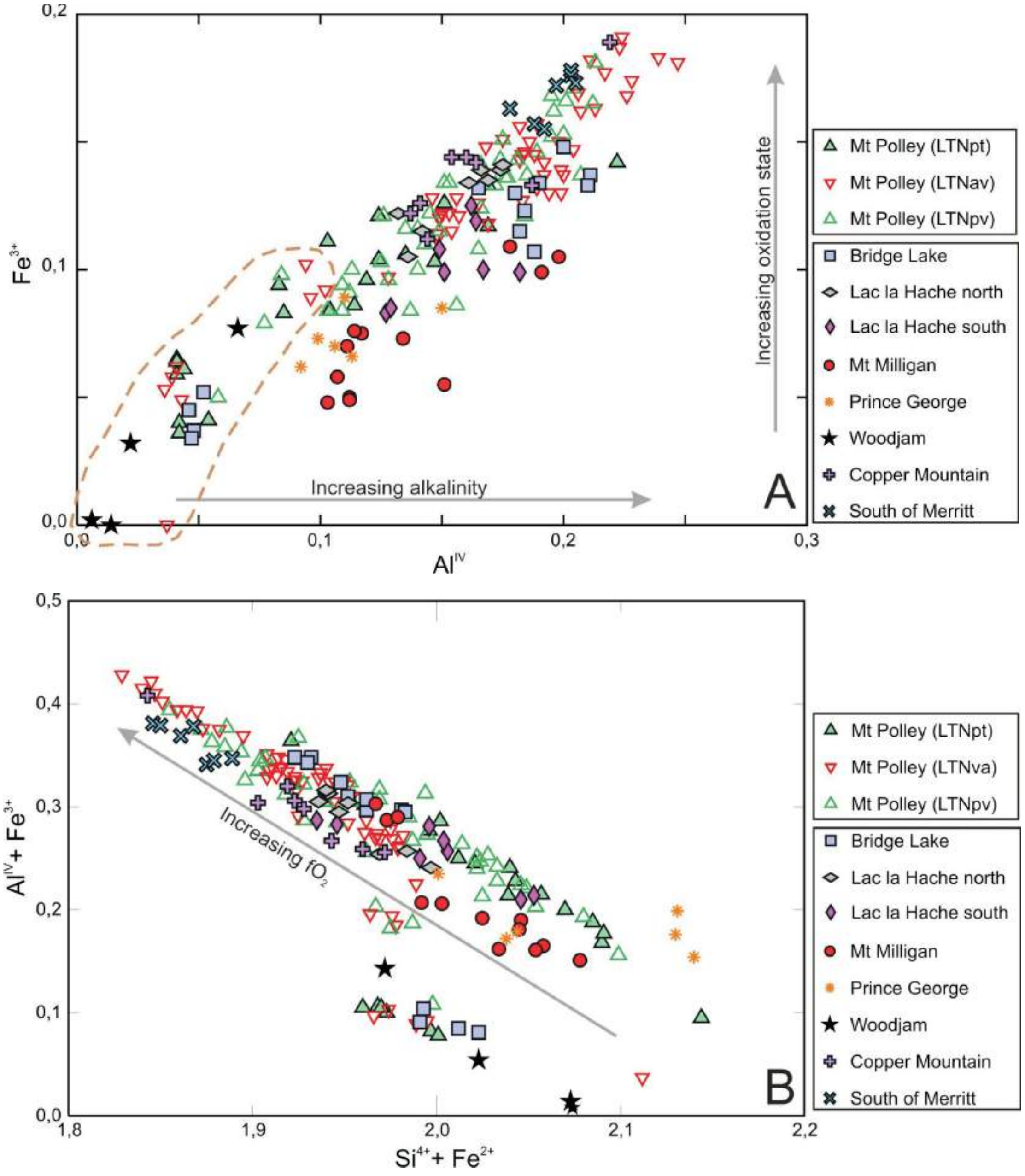

Figure 6. Cation relationships for clinopyroxene crystals from samples of Nicola Group basalts: **A)** direct relationship between Al^{IV} and Fe^{3+} in pyroxene composition from core to rim; **B)** negative correlation between ($Si^{4+} + Fe^{2+}$) and ($Al^{IV} + Fe^{3+}$) in pyroxene indicating higher oxygen fugacity (FO_2) with lower $Si^{4+} + Fe^{2+}$. Dashed brown line outlines pyroxene analyses from Woodjam, with some core and interior analyses from Bridge Lake and Mount Polley.

higher calculated Fe^{3+} (~0.10–0.19 cpfu) and Al^{IV} (~0.13–0.25 cpfu) content, compared with Fe^{3+} (0.002–0.13 cpfu) and Al^{IV} (0.006–0.15 cpfu) from the Mount Milligan, Mount Polley unit LTNpt, Lac la Hache south, Prince George and Woodjam samples. Some analyses (core and interiors) of clinopyroxene from Bridge Lake and from all units at Mount Polley also belong to this latter group (Figure 6A, bottom left).

The Al^{IV} values increase directly proportional to Fe^{3+} contents (Figure 6A), but (Si^{4+} + Fe^{2+}) and (Al^{IV} + Fe^{3+}) show negative correlation (Figure 6B). These data suggest that clinopyroxene from samples obtained from Copper Mountain, Bridge Lake (rims), Lac la Hache north, LTNav and LTNpv units near Mount Polley and south of Merritt crystallized from a melt with higher relative oxygen fugacity than the others.

Fe-Ti–Oxide Minerals

Primary Fe-Ti–oxide minerals are commonly present as inclusions within clinopyroxene in the study area. These oxides exhibit subsolidus exsolution features, and distinctive compositions and textures (Figure 7). Representative analyses of primary Fe-Ti oxides show variable Fe^{3+}, Ti and Fe^{2+} contents (Figure 8). A few spot analyses in exsolution lamellae within crystals from the LTNpt unit at Mount Polley (Figure 7C), Lac la Hache south and Prince George are depleted in Fe^{3+} and relatively enriched in Ti. The former plots within the ferropseudobrookite and ilmenite fields respectively; the latter plots within the ulvoespinel field (Figure 8).

The remaining spot analyses from Lac la Hache south and Prince George samples show titanomagnetite compositions, while the remaining spots from the LTNpt unit span from titanomagnetite to maghemite (cation-deficient spinel) compositions (Figure 8). The Fe-Ti oxides from Mount Milligan plot as a relatively Fe^{2+}-rich magnetite. The other crystals analyzed from samples of Mount Polley LTNav and LTNpv units, Bridge Lake, Lac la Hache north, Copper Mountain, south of Merritt and Woodjam tend to increase the ferric iron content, falling in the titanomagnetite, magnetite and maghemite fields.

Discussion and Conclusions

The results presented above show some systematic differences among the basalts studied, on the basis of pyroxene and Fe-Ti–oxide chemistry. The EMP analyses from core to rim in clinopyroxene from the Woodjam area presents high Mg# and SiO_2%, low Fe and Al cpfu values (Figures 5 and 6A) relative to those from samples collected in the other areas. This denotes a relatively homogeneous, primitive and reduced magma chamber. Some spot analyses in the core and interiors of pyroxene crystals from the Bridge Lake and Mount Polley areas are similar in composition to those at Woodjam. However, at Bridge Lake and Mount Polley the chemistry varies from core to rim, indicating a pyroxene fractionation trend, where the cores are richer in Mg and Si and poorer in Fe, Ti and Al than the rims, which suggests a rapid change in the temperature-composition (T-X) param-

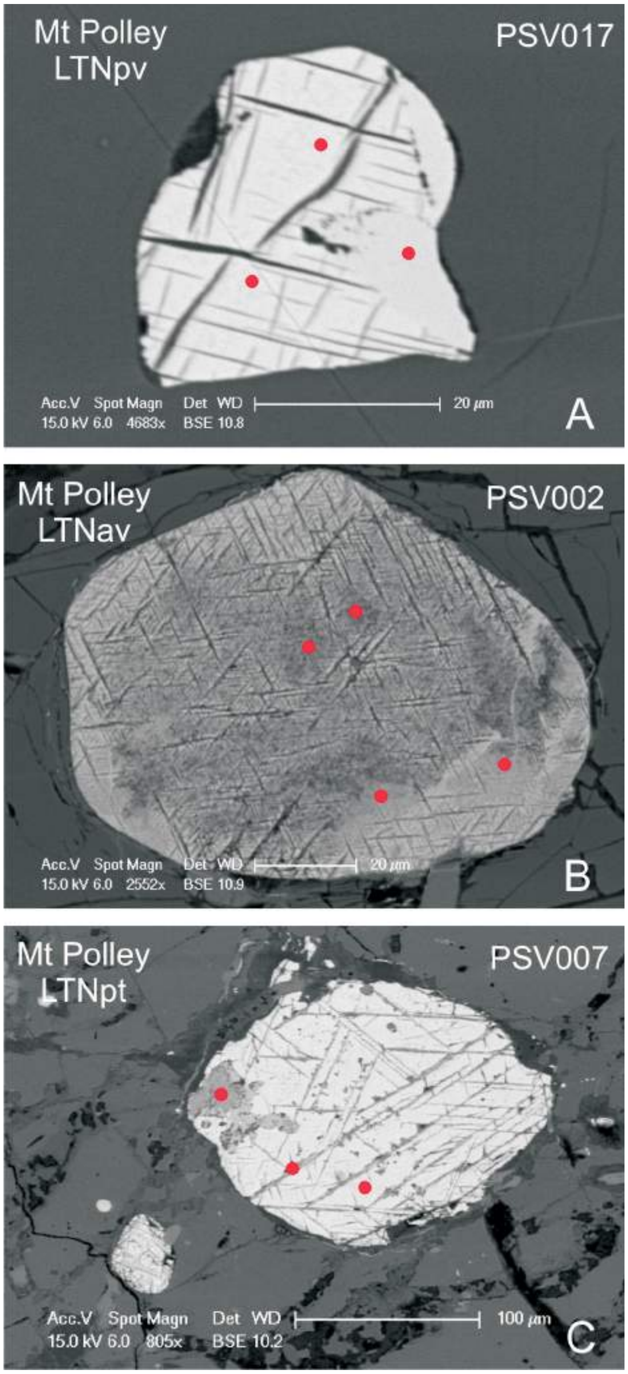

Figure 7. Representative backscattered electron images of Fe-Ti–oxide minerals; electron microprobe (EMP) analysis spots are shown in red: **A)** magnetite with lamellae of titanomagnetite, maghemite at the border of the grain (right side of the crystal); **B)** magnetite composition in the core (dark gray) and titanomagnetite composition at the border (light gray) of the crystal; **C)** Ferropseudobrookite lamellae (dark gray) within titanomagnetite grain (light gray).

eters during crystallization. Thus, the Bridge Lake sample and a few samples from Mount Polley suggest a transition from a primitive, relatively reduced and less alkaline magma, to a less primitive, relatively oxidized and more alkaline one.

The Al and Fe^{3+} contents in pyroxene are indicators of the alkalinity and the oxygen fugacity of magma (Kushiro, 1960; LeBas, 1962), respectively. Pyroxene from Copper Mountain, Bridge Lake, Lac la Hache north, LTNav and LTNpv units at Mount Polley and south of Merritt, is more alkaline, and crystallized at higher oxygen fugacity, than the pyroxene crystals around the Mount Milligan, unit LTNpt at Mount Polley, Lac la Hache south, Prince George and Woodjam areas (Figure 6A and B). This is consistent with the findings of Mortimer (1987), where pyroxenes from his alkalic type 1 basalts plot in the diopside field and thus in the same area as most samples presented herein, whereas calcalkalic and transitional tholeiitic lavas contain augitic clinopyroxene.

Chemistry of Fe-Ti–oxide inclusions in pyroxene can be grouped into two populations. The first one corresponds to crystals relatively rich in Fe^{3+}, such as magnetite and maghemite from LTNpv and LTNav units at Mount Polley, Bridge Lake, Lac la Hache north, Copper Mountain, south of Merritt and Woodjam (Figure 8). The second group corresponds to grains relatively rich in Ti and Fe^{2+}, typically titanomagnetite, showing subsolidus exsolution lamellae of ferropseudobrookite, ilmenite and ulvoespinel, denoting relatively reduced conditions of formation. Samples from unit LTNpt at Mount Polley, Mount Milligan, Lac la Hache south and Prince George belong to this group (Figure 8).

The results presented above are consistent with the oxidation states inferred from the pyroxene composition, with the exception of Fe-Ti oxides at Woodjam, which are Fe^{3+} rich, potentially due to a late alteration process as indicated by secondary hematite affecting the groundmass of the rock (Table 2).

This research shows that the oxidation state predicted from Fe-Ti–oxide chemistry is not proportional to the magnetic susceptibility of the rock (Table 2). The Fe-Ti–oxide minerals have variable magnetic susceptibility values (Hunt et al., 1995; Peters and Dekkers, 2003) because the magnetic susceptibility of the rock depends on the abundance as well as type of Fe-Ti minerals.

Comparing the petrographic description of the collected samples with the chemical composition of pyroxene and Fe-Ti oxides, it can be concluded that pyroxene and pyroxene-analcime–bearing basalts of the Quesnel terrane were produced from a more oxidized magma than pyroxene-plagioclase–rich basalts.

Considering the petrography and pyroxene plus Fe-Ti–oxide geochemistry, it can be implied that basalts of Copper

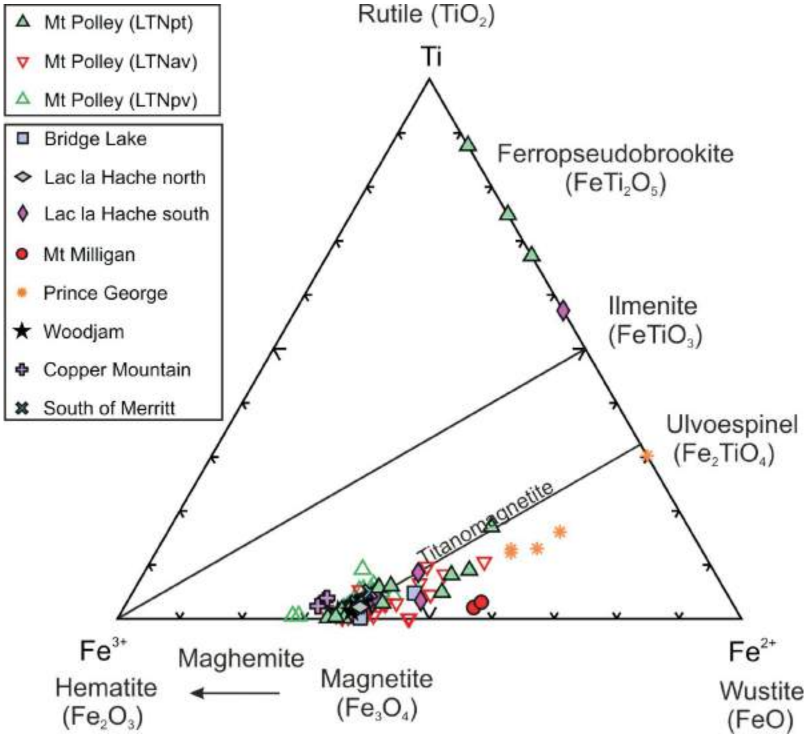

Figure 8. The Fe^{3+}-Ti-Fe^{2+} cpfu (cations per formula unit) contents of Fe-Ti–oxide minerals as inclusions in pyroxene crystals of the Nicola Group, British Columbia, plotted in FeO-Fe_2O_3-TiO_2 space after the method of Taylor (1964).

Mountain, Lac la Hache north, units LTNav and LTNpv at Mount Polley, and south of Merritt represent similar magma-generating conditions that were likely oxidized and relatively alkaline. Such rocks are found in spatial and temporal proximity to porphyry mineralization at Mount Polley and Copper Mountain. Thus, the magmatic chambers source of the volcanic rocks around south of Merritt, and Lac la Hache north, may also have had the potential to develop comagmatic porphyry-style mineralization.

The Bridge Lake area might represent a transition between reduced and oxidized magma, while the unit LTNpt at Mount Polley, Lac la Hache south, Prince George and Woodjam may be the evidence of a reduced magma-generating environment. The sources of these lavas had probably less potential to evolve in a fertile intrusion.

This research is based on the mineral chemistry of basalt. To produce porphyry mineralization, a change in the tectonic setting that results in intrusive rather than extrusive magmatism is necessary. However, our work suggests that indications for a favourable magma-generating environment are also recorded in the precursor volcanic rocks in prospective arc segments.

Acknowledgments

Geoscience BC is thanked for the economic support to this project. The authors also acknowledge E. Czech and J. Lai for their help in the SEM-EMP laboratory during sample preparation and data acquisition. The peer review and comments provided by M. Mihalynuk helped to improve clarity of this paper.

References

Bailey, D.G. and Hodgson C, J. (1979): Transported altered wall rock in laharic breccias at the Cariboo-Bell Cu-Au porphyry deposit, British Columbia; Economic Geology, v. 74, p. 125–12, URL <http://econgeol.geoscienceworld.org/cgi/reprint/ 74/1/125.pdf> [November 2011].

Bissig, T., Vaca, S., Schiarizza, P. and Hart, C. (2010): Geochemical and physical variations in the Late Triassic Nicola Arc and metallogenic implications, central British Columbia (NTS 092P, 093A, N): preliminary results; *in* Geoscience BC Summary of Activities 2009, Geoscience BC, Report 2010-1, p. 49–52, URL <http://www.geosciencebc.com/i/pdf/SummaryofActivities2009/SoA2009_Bissig.pdf> [November 2011].

Blackwell, J., Lesage, G., Skinner, T., Eckfeldt, M., Hamilton, J., Hertel, J., Laird, B., Madsen, J., Rainbow, A., Sherlock, R. and Sepp, M. (2010): Woodjam property mapping 2010 interpretation, geology of the Woodjam property core area; unpublished internal report, Gold Fields Canada Exploration.

Carter, E.S., Orchard, M.J., Ross, C.A., Ross, J.R.P., Smith, P.L. and Tipper, H.W. (1991): Geology of the Cordillera Orogen in Canada, Part B, paleontological signatures of terranes; Chapter 2 *in*, H. Gabrielse and C.J. Yorath (ed.), Geological Survey of Canada, Geology of Canada, no. 4, p. 28–38 and The Geology of North America; Geological Society of America, v. G-2.

Chamberlain, C.M., Jackson, M., Jago, C.P., Pass, H.E., Simpson, K.A., Cooke, D.R. and Tosdal, R.M. (2007): Toward an integrated model for alkalic porphyry copper deposits in British Columbia (NTS 093A, N; 104G); *in* Geoscience BC Summary of Activities 2006, Geoscience BC, Report 2007-1, p. 259–274, URL <http://www.empr.gov.bc.ca/Mining/Geoscience/PublicationsCatalogue/Fieldwork/Documents/26-Chamberlain.pdf> [November 2011].

Dawson, G.M. 1879: Preliminary report on the physical and geological features of the southern portion of the interior of British Columbia, 1877; Geological Survey of Canada, Progress Report, 1877–1878, p. 96B-101B.

Droop, G.T.R. (1987) A general equation for estimating Fe^{3+} concentrations in ferromagnesian silicates and oxides from microprobe analyses, using stoichiometric criteria; Mineralogical Magazine, v. 51, p 431–435.

Hunt, C.P., Moskowitz, B. M. and Banerjee, S. K. (1995): Magnetic properties of rocks and minerals; *in* Rock Physics and Phase Relations: A Handbook of Physical Constants, T.J Ahrens (ed.), AGU Reference Shelf 3, American Geophysical Union, p. 189–204.

Kushiro, I. (1960): Si-Al relations in clinopyroxenes from igneous rocks; American Journal of Science, v. 258, p. 548–554.

LeBas, M.J. (1962): The role of aluminum in igneous clinopyroxenes with relation to their parentage; American Journal of Science, v. 260, p. 267–288.

Logan, J.M. and Bath, A.B. (2005): Geochemistry of Nicola Group basalt from the central Quesnel trough at the latitude of Mount Polley (NTS 093A/5, 6, 11, 12), central British Columbia; *in* Geological Fieldwork, BC Ministry of Energy and Mines, Paper 2006-1, p. 83–98, URL <http://www.empr.gov.bc.ca/Mining/Geoscience/PublicationsCatalogue/Fieldwork/Documents/2005/Paper09.pdf> [November 2011].

Logan, J.M., Bath, A., Mihalynuk, M.G. and Rees, C.J. (2007): Regional geology of the Mount Polley area, central British Columbia; BC Ministry of Energy and Mines, Geoscience Map 2007-1, scale 1:50 000, URL <http://www.em.gov.bc.ca/Mining/Geoscience/PublicationsCatalogue/Maps/GeoscienceMaps/Documents/GM2007-1_Mount_Polley.pdf> [November 2011].

Logan, J.M., Mihalynuk, M.G., Friedman, R.M. and Creaser, R.A. (2011): Age constraints of mineralization at the Brenda and Woodjam Cu-Mo±Au porphyry deposits - an Early Jurassic calcalkaline event, south-central British Columbia; *in* Geological Fieldwork 2010, BC Ministry of Energy and Mines, Paper 2011-1, p. 129–144, URL <http://www.fjordlandex.com/Research/2010Fieldwork.pdf> [November 2011].

Morimoto, N., Fabries, J., Ferguson, A.K., Ginzburg, I.V., Ross, M., Seifert, F.A., Zussman, J., Aoki, K. and Gottardi, G. (1988): Nomenclature of pyroxenes; American Mineralogist, v. 173, p. 1123–1133, URL <http://www.minsocam.org/ammin/AM73/AM73_1123.pdf> [November 2011].

Mortensen, J.K., Ghosh, D.K. and Ferri, F. (1995): U-Pb geochronology of intrusive rocks associated with copper-gold porphyry deposits in the Canadian Cordillera; *in* Porphyry Deposits of the Northwestern Cordillera of North America, T.G. Schroeter (ed.), Canadian Institute of Mining, Metallurgy and Petroleum, Special Volume 46, p. 142–158.

Mortimer, N. (1987): The Nicola Group: Late Triassic and Early Jurassic subduction-related volcanism in British Columbia; Canadian Journal of Earth Sciences, v. 24, p. 2521–2536.

Nelson, J.L. and Bellefontaine, K.A. (1996): The geology and mineral deposits of north-central Quesnellia; Tezzeron Lake to Discovery Creek, central British Columbia; BC Ministry of Energy and Mines, Bulletin 99, 100 p, URL <http://www.empr.gov.bc.ca/Mining/Geoscience/PublicationsCatalogue/BulletinInformation/BulletinsAfter1940/Documents/Bulletin_099.pdf> [November 2011].

Peters, C. and Dekkers, M.J. (2003): Selected room temperature magnetic parameters as a function of mineralogy, concentration and grain size; Physics and Chemistry of the Earth, v. 28, no. 16–19, p. 659–667.

Pouchou, J.L. and Pichoir, F. (1985): "PAP" $\phi(\rho Z)$ procedure for improved quantitative microanalysis; *in* Microbeam Analysis -1985, J.T. Armstrong (ed.), San Francisco Press, p. 104–106.

Preto, V.A. (1979): Geology of the Nicola Group between Merritt and Princeton; BC Ministry of Energy and Mines, Bulletin 69, 90 p., URL <http://www.em.gov.bc.ca/Mining/Geoscience/PublicationsCatalogue/BulletinInformation/BulletinsAfter1940/Documents/Bulletin_069.pdf> [November 2011].

Schiarizza, P., Bligh, J., Bluemel, B. and Tait, D. (2008): Geology of the Timothy Lake Area (NTS 092P/14); BC Ministry of Energy and Mines, Open File, 2008-5, 1:50 000 scale, URL <http://www.empr.gov.bc.ca/Mining/Geoscience/PublicationsCatalogue/OpenFiles/2008/Pages/2008-5.aspx> [November 2011].

Seedorff, E., Dilles, J.H., Proffett, J.M., Jr., Einaudi, M.T., Zurcher, L., Stavast, W.J.A., Johnson, D. and Barton, M.D. (2005): Porphyry deposits: characteristics and origin of hypogene features; Economic Geology, 100th Anniversary Volume, p. 251–298.

Taylor, R. W. (1964): Phase equilibriums in the system FeO-Fe_2O_3-TiO_2 at 1300°C; American Mineralogist, v. 49, no. 7–8, p. 1016–1030.

Vaca, S., Bissig, T., Mitchinson, D.F., Barker, S. and Hart, C.J.R. (2011): Variability in the basaltic rocks hosting Cu-Au porphyry mineralization in the Quesnel terrane, south-central British Columbia (NTS 092, 093): geochemistry, stable isotopes and physical properties; *in* Geoscience BC Summary of Activities 2010, Geoscience BC, Report 2011-1, p. 123–132, URL <http://www.geosciencebc.com/i/pdf/SummaryofActivities2010/SoA2010_Vaca_etal.pdf> [November 2011].